

Status of Neutrino Fits

C. Giunti

*INFN, Sezione di Torino, and Dipartimento di Fisica Teorica,
Università di Torino, Via P. Giuria 1, I-10125 Torino, Italy*



I review the current status of solar, KamLAND, atmospheric and K2K neutrino experiments, implications for three-neutrino mixing and upper bounds for the neutrino masses.

1 Introduction

The last five years have been extraordinary for neutrino physics, with the Super-Kamiokande evidence of atmospheric neutrino oscillations¹, the SNO evidence of solar neutrino oscillations^{2,3}, the KamLAND⁴ and K2K⁵ confirmations of these evidences with neutrinos from controlled laboratory sources. As a result of the findings of these and other important experiments, a scenario of bilarge mixing of three neutrinos has emerged as favored by the data.

In this review I briefly summarize the results of solar, KamLAND, atmospheric and K2K neutrino experiments in Sections 2 and 3 and their interpretation in terms of two-neutrino oscillations. In Section 4 I describe the three-neutrino mixing schemes favored by neutrino oscillation data and I discuss the open problem of the determination of the absolute neutrino mass scale, including the recent stringent limit⁶ from cosmological data. Conclusions are drawn in Section 5.

2 Solar Neutrino Experiments and KamLAND

The Solar Neutrino Problem consists in a deficit of electron neutrinos arriving on Earth with respect to the flux predicted by the Standard Solar Model⁷ (SSM). It was discovered in the Homestake experiment⁸ in the late 60's and later confirmed by the Kamiokande⁹, SAGE¹⁰, GALLEX¹¹, GNO¹², Super-Kamiokande¹³ and SNO³ experiments. Table 1 shows the main characteristics of the rates measured in solar neutrino experiments. One can see that all the

Experiment	Reaction	E_{th} (MeV)	ν Flux Sensitivity	Operating Time	$\frac{R^{\text{exp}}}{R^{\text{BP2000}}}$
SAGE	CC: $\nu_e + {}^{71}\text{Ga} \rightarrow {}^{71}\text{Ge} + e^-$	0.233	$pp, {}^7\text{Be}, {}^8\text{B},$ $pep, hep,$ ${}^{13}\text{N}, {}^{15}\text{O}, {}^{17}\text{F}$	1990 – 2001	0.55 ± 0.05 ¹⁰
GALLEX				1991 – 1997	0.61 ± 0.06 ¹¹
GNO				1998 – 2000	0.51 ± 0.08 ¹²
Homestake	CC: $\nu_e + {}^{37}\text{Cl} \rightarrow {}^{37}\text{Ar} + e^-$	0.814	${}^7\text{Be}, {}^8\text{B},$ $pep, hep,$ ${}^{13}\text{N}, {}^{15}\text{O}, {}^{17}\text{F}$	1970 – 1994	0.34 ± 0.03 ⁸
Kamiokande	ES: $\nu + e^- \rightarrow \nu + e^-$	6.75	${}^8\text{B}$	1987 – 1995 2079 days	0.55 ± 0.08 ⁹
Super-Kam.		4.75		1996 – 2001 1496 days	0.465 ± 0.015 ¹³
SNO	CC: $\nu_e + d \rightarrow p + p + e^-$	6.9		1999 – 2002 306.4 days	0.35 ± 0.02 ³
	NC: $\nu + d \rightarrow p + n + \nu$	2.2			1.01 ± 0.13 ³
	ES: $\nu + e^- \rightarrow \nu + e^-$	5.2			0.47 ± 0.05 ³

Table 1: Main characteristics of the rates measured in solar neutrino experiments. CC = Charged Current; NC = Neutral Current; ES = Elastic Scattering; E_{th} = Energy threshold. The last column shows the measured rate normalized to the BP2000¹⁴ Standard Solar Model (SSM) prediction.

experiments measuring exclusively^a or mainly^b electron neutrinos observe a suppression between about 1/3 and 1/2 of the electron neutrino flux with respect to the BP2000¹⁴ SSM prediction.

In 2001² the SNO experiment measured the solar neutrino flux through the CC and ES reactions listed in Table 1. A comparison of the SNO CC rate and the Super-Kamiokande ES rate (which is compatible with the SNO ES rate, but more precise because of higher statistics) allowed the SNO Collaboration to claim a first 3.3σ evidence in favor of $\nu_e \rightarrow \nu_{\mu,\tau}$ transitions in the solar neutrino flux. The $\nu_{\mu,\tau}$ produced in these transitions interact through the ES reaction causing an increase of the ES rate with respect to the CC rate, normalized to the SSM prediction.

In 2002³, the observation by the SNO experiment of a rate compatible with the SSM prediction through the NC reaction marked the triumph of the SNO experiment, allowing the SNO Collaboration to proof the existence of $\nu_e \rightarrow \nu_{\mu,\tau}$ transitions in the solar neutrino flux using only its own data, simply by the comparison of the fluxes measured through the CC and NC reactions: $\Phi_{\nu_{\mu,\tau}}^{\text{SNO}} = \Phi_{\text{NC}}^{\text{SNO}} - \Phi_{\text{CC}}^{\text{SNO}} = (3.33 \pm 0.65) \times 10^6 \text{ cm}^{-2} \text{ s}^{-1}$. The model-independent evidence in favor of $\nu_e \rightarrow \nu_{\mu,\tau}$ transitions is at the level of 5.1σ . Moreover, the total flux of active neutrinos measured in the SNO NC reaction is perfectly compatible with the SSM flux, providing a strong evidence in favor of the correctness of the SSM (that was questioned before) and restricting possible transitions of solar ν_e 's into sterile neutrinos.

The SNO measurements have solved the long-standing Solar Neutrino Problem proving that it is due to new neutrino physics, because no astrophysical explanation can generate the observed $\nu_{\mu,\tau}$'s.

The simplest known explanation of the appearance of $\nu_{\mu,\tau}$ in the solar neutrino flux is neutrino oscillations due to neutrino mixing^c: the left-handed neutrino fields $\nu_{\alpha L}$ ($\alpha = e, \mu, \tau$),

^aThe radiochemical experiments Homestake⁸, SAGE¹⁰, GALLEX¹¹, GNO¹².

^bThe cross section of ν_e in the ES reaction in Kamiokande, Super-Kamiokande and SNO is about six times larger than the cross section of $\nu_{\mu,\tau}$. In the discussion of solar neutrino experiments ν_{μ} and ν_{τ} are considered together, because they are indistinguishable due to the low energy that does not allow charged-current reactions with production of μ or τ .

^cB. Pontecorvo discovered neutrino oscillations in 1958-59^{15,16} and worked on the theory and phenomenology

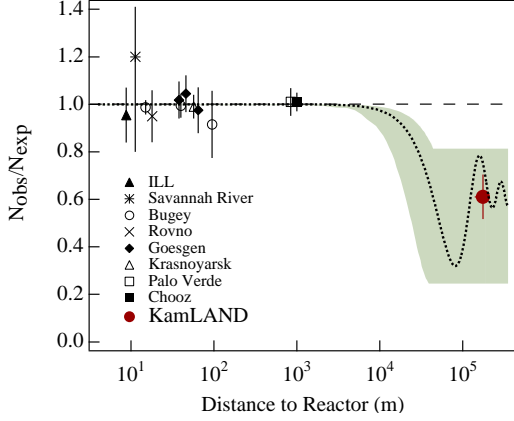


Figure 1: Ratio of measured to expected $\bar{\nu}_e$ flux in reactor experiments⁴. The shaded region (dotted curve) corresponds to the 95% C.L. LMA region (best-fit)²³.

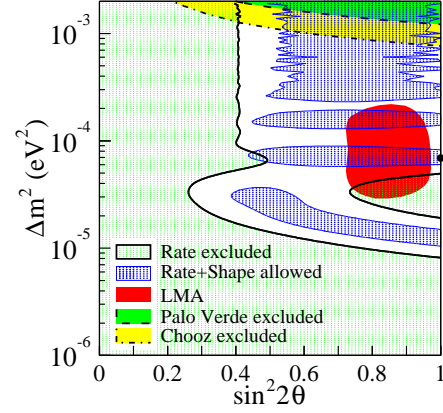


Figure 2: KamLAND⁴ excluded and allowed regions at 95% C.L. ($\theta = \vartheta_{\text{SUN}}$ and $\Delta m^2 = \Delta m_{\text{SUN}}^2$). The dark area is the 95% C.L. LMA region²³. The thick dot is the best fit of KamLAND data.

which appear in the weak charged current $j_{\rho}^{\text{CC}} = 2 \sum_{\alpha=e,\mu,\tau} \bar{\nu}_{\alpha L} \gamma_{\rho} \alpha$, are mixings of the neutrino fields ν_k with masses m_k ($k = 1, 2, 3, \dots$) according to the relation $\nu_{\alpha L} = \sum_k U_{\alpha k} \nu_{kL}$, where U is the unitary mixing matrix. The modification of the oscillation probability due to neutrino propagation in the Sun and the Earth (MSW effect^{21,22}) must be taken into account.

The data of solar neutrino experiments have been analyzed in several papers (see Ref. 24 and references therein) in terms of two-neutrino $\nu_e \rightarrow \nu_{\mu,\tau}$ oscillations, leading to a rather compelling indication in favor of the so-called LMA region in the plane of the mixing parameters $\tan^2 \vartheta_{\text{SUN}}$, Δm_{SUN}^2 (ϑ_{SUN} is the effective two-neutrino mixing angle and Δm_{SUN}^2 is the squared mass difference; see Refs. 17,25), at $\tan^2 \vartheta_{\text{SUN}} \approx 0.4$ and $\Delta m_{\text{SUN}}^2 \approx 5 \times 10^{-5} \text{ eV}^2$.

In December 2002 the KamLAND Collaboration published a spectacular confirmation of the LMA region obtained with their long-baseline reactor $\bar{\nu}_e$ oscillation experiment⁴ (see also the contribution of K. Inoue in these Proceedings). As shown in Fig. 1, KamLAND is the first reactor experiment that finds a suppression of the measured $\bar{\nu}_e$ flux with respect to the original one, thanks to the larger source-detector distance. The measured suppression is $R_{\text{KamLAND}}^{\bar{\nu}_e} = 0.611 \pm 0.085 \pm 0.041$. Figure 2 shows the regions in the $\sin^2 2\vartheta_{\text{SUN}} - \Delta m_{\text{SUN}}^2$ plane allowed by the KamLAND data. One can see that there are two areas of overlap with the LMA region obtained from solar neutrino data. Therefore, the KamLAND result is perfectly compatible with solar neutrino data and one can expect that a combined fit would yield two allowed subareas of the LMA region. Indeed, this is what happens, as shown in Fig. 3²⁶ (see Ref. 24 and references therein for similar results obtained by other authors). The best-fit point is²⁶

$$\tan^2 \vartheta_{\text{SUN}} \simeq 0.46, \quad \Delta m_{\text{SUN}}^2 \simeq 6.9 \times 10^{-5} \text{ eV}^2, \quad (2.1)$$

and $0.29 < \tan^2 \vartheta_{\text{SUN}} < 0.86$ at 99.73% C.L.

Figure 4²⁷ shows that the fraction of transitions of solar ν_e 's into sterile neutrinos, given by $\sin^2 \eta$, is limited ($\sin^2 \eta < 0.52$ at 3σ), and the measured total flux of solar ^8B neutrinos is in perfect agreement with the one predicted by the SSM, $\Phi_{^8\text{B}} = 1.00 \pm 0.06 \Phi_{^8\text{B}}^{\text{SSM}}$.

The increase of statistics of KamLAND data will hopefully allow to distinguish among the two LMA regions shown in Fig. 3 in the near future (see the contribution of K. Inoue in these

of neutrino oscillations for many years (see the review in Ref. 17). It is interesting to notice that Pontecorvo predicted a possible suppression of the solar electron neutrino flux in 1967¹⁸, before the first data of the Homestake experiment, which was aimed at the observation of solar ^8B in order to check the thermonuclear origin of the Sun energy^{19,20}.

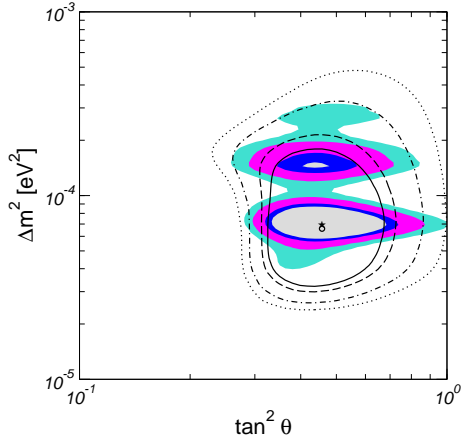


Figure 3: Allowed 90%, 95%, 99%, 99.73% (3σ) C.L. regions obtained from the fit of solar and KamLAND data²⁶ ($\theta = \vartheta_{\text{SUN}}$ and $\Delta m^2 = \Delta m_{\text{SUN}}^2$). The lines delimit the allowed regions from solar data.

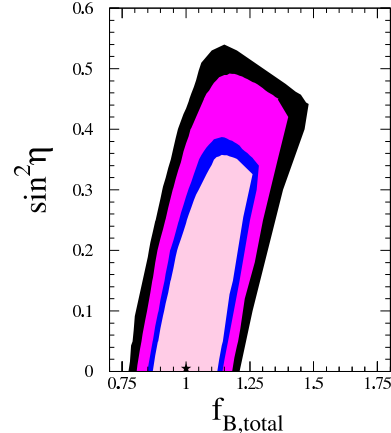


Figure 4: Allowed 90%, 95%, 99%, 99.73% (3σ) C.L. regions²⁷ in the $f_{\text{B,total}} - \sin^2 \eta$ plane, where $f_{\text{B,total}} = \Phi_{\text{sB}} / \Phi_{\text{sB}}^{\text{SSM}}$ and $\sin^2 \eta$ is the fraction of sterile neutrinos in the solar flux.

Proceedings).

3 Atmospheric Neutrino Experiments and K2K

In 1998 the Super-Kamiokande experiment discovered¹ an up-down asymmetry of high-energy events generated by atmospheric ν_μ 's, confirming the atmospheric neutrino anomaly discovered about ten years earlier by the Kamiokande²⁸ and IMB²⁹ experiments.

Cosmic rays interacting with nuclei in the atmosphere produce pions, which decaying produce muons and neutrinos. The muons that decay before hitting the ground produce more neutrinos. These neutrinos from pion and muon decay in the atmosphere are called “atmospheric neutrinos”. In the late 80's the Kamiokande and IMB experiments discovered an anomaly in the ratio of events produced by muon and electron neutrinos with respect to the calculated one³⁰, that indicated a disappearance of atmospheric muon neutrinos.

From simple geometry, the fluxes of high energy neutrinos (whose parent cosmic rays are not deflected by the magnetic field of the Earth) coming from above and below are equal. The 7σ Super-Kamiokande up-down asymmetry of high-energy ν_μ events, $A_\mu = [(U - D) / (U + D)]_\mu = -0.311 \pm 0.043 \pm 0.01$, is a model-independent proof of the disappearance of atmospheric muon neutrinos generated on the other side of the Earth.

The simplest explanation of the disappearance of atmospheric muon neutrinos is neutrino oscillations. The hypothesis of $\nu_\mu \rightarrow \nu_\tau$ transitions provides the best fit of the atmospheric neutrino data (the $\nu_\mu \leftrightarrow \nu_e$ channel is practically excluded and the $\nu_\mu \rightarrow \nu_s$ channel is strongly disfavored)³¹. The data of the Soudan-2³² and MACRO³³ atmospheric neutrino experiments confirm this interpretation, albeit with less precision than the Super-Kamiokande experiment.

The regions in the $\sin^2 2\vartheta_{\text{ATM}} - \Delta m_{\text{ATM}}^2$ plane allowed by Super-Kamiokande atmospheric neutrino data are shown in Fig. 5: the small regions centered around the best-fit point

$$\sin^2 2\vartheta_{\text{ATM}} = 1, \quad \Delta m_{\text{ATM}}^2 = 2.5 \times 10^{-3} \text{ eV}^2. \quad (3.1)$$

The oscillation explanation of the disappearance of atmospheric muon neutrinos has been recently confirmed in the long-baseline accelerator K2K experiment⁵ in which muon neutrinos are produced in a laboratory by pion decay. The K2K experiment measured 56 events instead of $80.1_{-5.4}^{+6.2}$ events expected in absence of oscillations, with a probability smaller than 1% that the suppression is due to a statistical fluctuation. The large allowed regions in Fig. 5, obtained

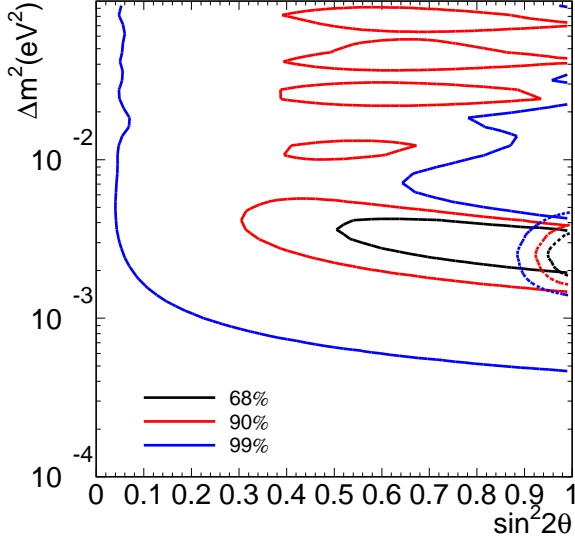


Figure 5: Allowed K2K regions (large) compared with the atmospheric Super-Kamiokande allowed regions (small regions)³⁶. $\theta = \vartheta_{\text{ATM}}$ and $\Delta m^2 = \Delta m_{\text{ATM}}^2$.

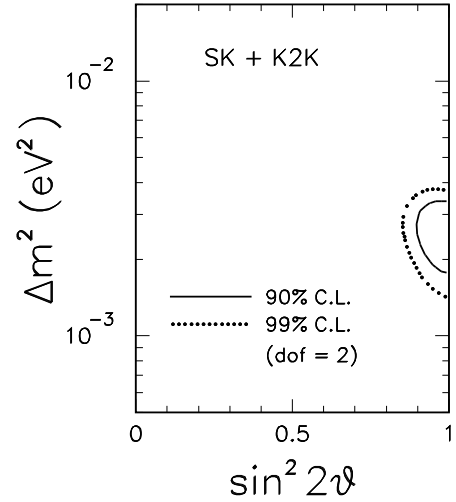


Figure 6: Regions allowed by a combined fit of the Super-Kamiokande atmospheric data and K2K data³⁴ ($\vartheta = \vartheta_{\text{ATM}}$ and $\Delta m^2 = \Delta m_{\text{ATM}}^2$).

from a two-neutrino oscillation fit of the K2K data, are in beautiful agreement with the Super-Kamiokande allowed regions from atmospheric data.

Figure 6 shows the allowed region in the $\sin^2 2\vartheta_{\text{ATM}} - \Delta m_{\text{ATM}}^2$ plane resulting from a combined fit of the Super-Kamiokande atmospheric data and K2K data³⁴. The main effect of the K2K data is to slightly lower the upper bound on Δm_{ATM}^2 , because a $\Delta m_{\text{ATM}}^2 \sim (4 - 6) \times 10^{-3} \text{ eV}^2$ would produce an unobserved suppression of the K2K energy spectrum peak³⁴.

In the near future K2K will take more data, hopefully confirming the agreement with the Super-Kamiokande evidence of atmospheric neutrino oscillations. Within some years the long-baseline accelerator experiments MINOS and CNGS will improve the precision of the determination of $\sin^2 2\vartheta_{\text{ATM}}$ and Δm_{ATM}^2 and will check the $\nu_{\mu} \rightarrow \nu_{\tau}$ explanation (see Ref.³⁵).

4 Three-Neutrino Mixing

The results of solar, KamLAND, atmospheric and K2K neutrino experiments can be explained comfortably by the hypothesis of three-neutrino mixing, which is the simplest and most natural one given our knowledge of the existence of only three active flavor neutrinos, ν_e , ν_{μ} and ν_{τ} ^d. Figure 7 shows the two three-neutrino schemes compatible with the hierarchy of solar and atmospheric Δm^2 's in Eqs. (2.1) and (3.1). Since the absolute scale of neutrino masses is not fixed by oscillation data, the two schemes allow a hierarchy (normal or inverted) of the neutrino masses if one mass is much smaller than the other two, or an almost degeneracy of the three neutrino masses, as shown in Figs. 8 and 9.

The hierarchy $\Delta m_{\text{SUN}}^2 \ll \Delta m_{\text{ATM}}^2$ implies that solar (and KamLAND) neutrino oscillations depend only on the first row of the mixing matrix (U_{e1} , U_{e2} , U_{e3}) and atmospheric (and K2K) neutrino oscillations depend only on the third column of the mixing matrix (U_{e3} , $U_{\mu 3}$, $U_{\tau 3}$).

^dAlthough the number of active flavor neutrinos is known to be three, the number of massive neutrinos could be larger than three, if there are sterile neutrinos (see Ref.²⁵). The additional massive neutrinos may be needed in order to generate a Δm^2 of the order of 1 eV necessary to explain the $\bar{\nu}_{\mu} \rightarrow \bar{\nu}_e$ transitions observed in the short-baseline LSND experiment³⁷. The existence of these transitions is under investigation in the MiniBooNE experiment³⁸.

Indeed, since ν_μ and ν_τ are indistinguishable in solar neutrino experiments (because of the low energy that allows only neutral-current interactions), solar neutrino oscillations can be expressed in terms of the probability of ν_e disappearance, which depends only on the elements U_{e1} , U_{e2} , U_{e3} of the mixing matrix. In the case of atmospheric neutrino oscillations, since $\Delta m_{\text{SUN}}^2 = \Delta m_{21}^2$ is too small to have any effect, ν_1 and ν_2 are indistinguishable and all probabilities depend on $|U_{\alpha 3}|^2 = 1 - |U_{\alpha 1}|^2 - |U_{\alpha 2}|^2$, for $\alpha = e, \mu, \tau$ (in other words, the oscillations are CP-invariant and do not depend on the mixing angle θ_{12} in the standard parameterization of the mixing matrix; see Ref. 39).

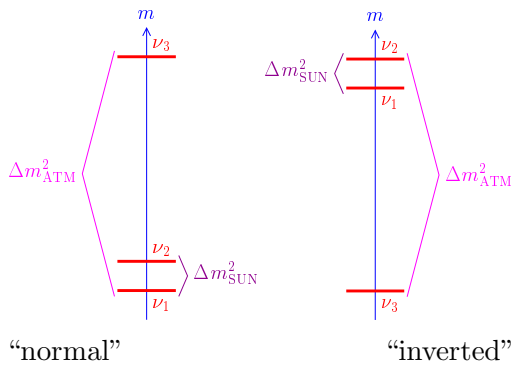


Figure 7: The two three-neutrino schemes allowed by the hierarchy $\Delta m_{\text{SUN}}^2 \ll \Delta m_{\text{ATM}}^2$. The massive neutrinos are labeled in order to have $\Delta m_{\text{SUN}}^2 = \Delta m_{21}^2$ and $\Delta m_{\text{ATM}}^2 = |\Delta m_{31}^2|$.

in terms of two-neutrino mixing give information on three-neutrino mixing.

Expressing the mixing angles measured in solar–KamLAND, atmospheric–K2K and CHOOZ–Palo Verde experiments in terms of the elements of the mixing matrix as $\sin^2 2\vartheta_{\text{SUN}} = 4|U_{e1}|^2|U_{e2}|^2$, $\sin^2 2\vartheta_{\text{ATM}} = 4|U_{\mu 3}|^2(1 - |U_{\mu 3}|^2)$, $\sin^2 2\vartheta_{\text{CH-PV}} = 4|U_{e3}|^2(1 - |U_{e3}|^2)$, the results of these experiments imply the so-called bilarge mixing matrix⁴⁴

$$|U| \simeq \begin{pmatrix} 0.70 - 0.87 & 0.50 - 0.69 & 0.00 - 0.16 \\ 0.20 - 0.61 & 0.34 - 0.73 & 0.60 - 0.80 \\ 0.21 - 0.63 & 0.36 - 0.74 & 0.58 - 0.80 \end{pmatrix}, \quad (4.1)$$

in which all the elements are large, except U_{e3} . In the future, the most pressing task is to measure the value of $|U_{e3}|$ (see the contribution of M. Mezzetto in these Proceedings), because if $|U_{e3}|$ is not too small, in future experiments it may be possible to distinguish between the normal and inverted schemes in Fig. 7 (through different matter effects) and to measure CP violation in neutrino oscillations.

Another important open question is the absolute value of neutrino masses (see Ref. 45). The Mainz and Troitsk tritium β -decay experiments provide the upper bound $m_{\nu_e} < 2.2 \text{ eV}$ (95% C.L.)⁴⁶ on the effective electron neutrino mass, which translates into an upper bound of 2.2 eV for all the three neutrino masses, because of the small Δm^2 's in Eqs. (2.1) and (3.1). In the future the KATRIN experiment⁴⁷ will explore m_{ν_e} down to about 0.3 eV.

A rather tight upper bound for the neutrino masses has been obtained very recently through a combined analysis of cosmological data, following the first results of the WMAP satellite experiment⁶ (see also the contribution of M. Limon in these Proceedings). The fit of Cosmic Microwave background (CMB) and Large Scale Structure (LSS) data in the framework of standard Big-Bang cosmology gives the upper bound

$$\sum_k m_k < 0.71 \text{ eV} \quad (95\% \text{ confidence}). \quad (4.2)$$

The only element of the mixing matrix that connects solar and atmospheric neutrino oscillations is U_{e3} . Therefore, any information on the value of U_{e3} is of crucial importance for the interpretation of solar and atmospheric neutrino data in the framework of three-neutrino mixing. Such very important information comes from the CHOOZ⁴⁰ and Palo Verde⁴¹ long-baseline reactor experiments, which did not observe any disappearance of $\bar{\nu}_e$'s through oscillations due to Δm_{ATM}^2 , leading to the upper bound $|U_{e3}|^2 < 5 \times 10^{-2}$ (99.73% C.L.)⁴². This limit is very important, because it means that solar and atmospheric neutrino oscillations are practically decoupled effective two-neutrino oscillations⁴³. Hence, the analyses of solar and atmospheric neutrino data

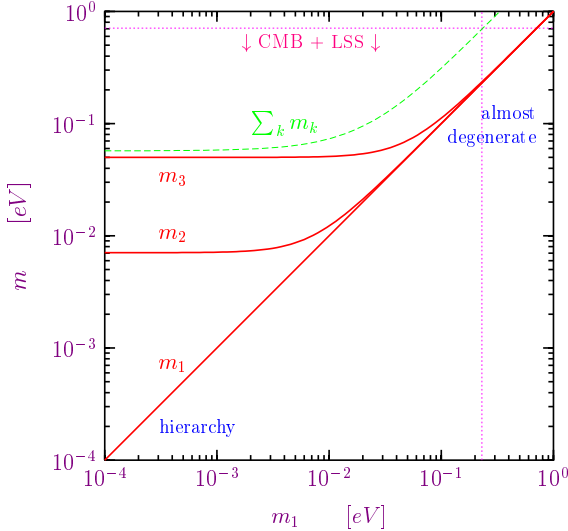


Figure 8: Values of the neutrino masses as functions of the lightest mass m_1 in the normal scheme in Fig. 7.

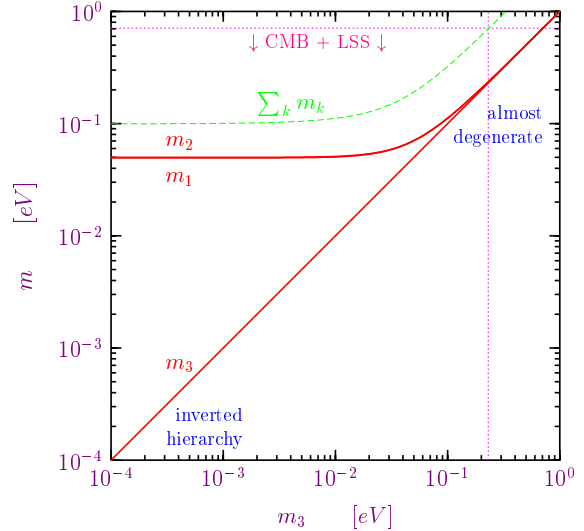


Figure 9: Values of the neutrino masses as functions of the lightest mass m_3 in the inverted scheme in Fig. 7.

This limit is shown by the horizontal dotted line in Figs. 8 and 9, with the sum of neutrino masses given by the dashed line. From these figures it is clear that the limit can be saturated only if the three neutrino masses are almost degenerate, in both normal and inverted schemes. Therefore, as shown by the vertical dotted line in Figs. 8 and 9, the cosmological upper limit on each neutrino mass is one third of that in Eq. (4.2): $m_k < 0.23 \text{ eV}$ (95% confidence). This upper bound is very impressive and appears already stronger than the sensitivity of about 0.3 eV of the future KATRIN experiment⁴⁷. Let me however emphasize that the KATRIN experiment is nevertheless very important to confirm the cosmological bound, which follows from several plausible but not certain assumptions. Even more interesting would be a measurement of a neutrino mass above the cosmological bound, which would demand a non-standard explanation.

5 Conclusions

We have seen that the last years have been exceptionally fruitful for neutrino physics. Important experimental discoveries give us a rather convincing picture of neutrino mixing. However, there are still important questions that need to be clarified:

1. Which is the absolute scale of neutrino masses? At present we have only upper bounds from direct measurements and from cosmological data.
2. Are neutrinos Dirac or Majorana particles? There is a strong experimental effort to detect neutrinoless double- β decay, whose existence would imply that neutrinos are Majorana particles (which is theoretically favored, especially in view of the see-saw mechanism).
3. Are the $\bar{\nu}_\mu \rightarrow \bar{\nu}_e$ transitions observed in the short-baseline LSND experiment³⁷ real? The answer will hopefully come soon from the MiniBooNE experiment³⁸.
4. Which is the number of massive neutrinos? If it is larger than three there may be transitions of active neutrinos into sterile states in oscillation experiments.
5. If the three-neutrino mixing scheme will be confirmed, is it normal or inverted? These two schemes may be distinguished in future long-baseline experiments through different matter effects if $|U_{e3}|$ is not too small. Eventually, the two schemes may be distinguished by a direct measurement of all three masses.

6. Is there CP violation in the lepton sector? The possibility to measure CP violation in future long-baseline experiments is currently under study (see the contribution of M. Mezzetto in these Proceedings).

In conclusion, I think that the future promises to be very interesting for neutrino physics.

References

1. Super-Kamiokande, Y. Fukuda et al., Phys. Rev. Lett. 81 (1998) 1562, hep-ex/9807003.
2. SNO, Q.R. Ahmad et al., Phys. Rev. Lett. 87 (2001) 071301, nucl-ex/0106015.
3. SNO, Q.R. Ahmad et al., Phys. Rev. Lett. 89 (2002) 011301, nucl-ex/0204008.
4. KamLAND, K. Eguchi et al., Phys. Rev. Lett. 90 (2003) 021802, hep-ex/0212021.
5. K2K, M.H. Ahn et al., Phys. Rev. Lett. 90 (2003) 041801, hep-ex/0212007.
6. D.N. Spergel et al., astro-ph/0302209.
7. J.N. Bahcall, AAPPS Bull. 12N4 (2002) 12, astro-ph/0209080.
8. Homestake, B.T. Cleveland et al., Astrophys. J. 496 (1998) 505.
9. Kamiokande, Y. Fukuda et al., Phys. Rev. Lett. 77 (1996) 1683.
10. SAGE, J.N. Abdurashitov et al., J. Exp. Theor. Phys. 95 (2002) 181, astro-ph/0204245.
11. GALLEX, W. Hampel et al., Phys. Lett. B447 (1999) 127.
12. GNO, M. Altmann et al., Phys. Lett. B490 (2000) 16, hep-ex/0006034.
13. Super-Kamiokande, S. Fukuda et al., Phys. Lett. B539 (2002) 179, hep-ex/0205075.
14. J.N. Bahcall et al., Astrophys. J. 555 (2001) 990, astro-ph/0010346.
15. B. Pontecorvo, Sov. Phys. JETP 6 (1957) 429, [Zh. Eksp. Teor. Fiz. 33, 549 (1957)].
16. B. Pontecorvo, Zh. Eksp. Teor. Fiz. 34 (1958) 247, [Sov. Phys. JETP 7, 172 (1958)].
17. S.M. Bilenky and B. Pontecorvo, Phys. Rept. 41 (1978) 225.
18. B. Pontecorvo, Zh. Eksp. Teor. Fiz. 53 (1967) 1717, [Sov. Phys. JETP 26, 984 (1968)].
19. J.N. Bahcall, Phys. Rev. Lett. 12 (1964) 300.
20. R. Davis, Phys. Rev. Lett. 12 (1964) 303.
21. L. Wolfenstein, Phys. Rev. D17 (1978) 2369.
22. S.P. Mikheev and A.Y. Smirnov, Nuovo Cim. C9 (1986) 17.
23. G.L. Fogli et al., Phys. Rev. D66 (2002) 053010, hep-ph/0206162.
24. C. Giunti and M. Laveder, hep-ph/0301276.
25. S.M. Bilenky et al., Prog. Part. Nucl. Phys. 43 (1999) 1, hep-ph/9812360.
26. M. Maltoni, T. Schwetz and J. Valle, hep-ph/0212129.
27. J.N. Bahcall et al., JHEP 0302 (2003) 009, hep-ph/0212147.
28. Kamiokande-II, K.S. Hirata et al., Phys. Lett. B280 (1992) 146.
29. R. Becker-Szendy et al., Phys. Rev. D46 (1992) 3720.
30. T.K. Gaisser and M. Honda, Ann. Rev. Nucl. Part. Sci. 52 (2002) 153, hep-ph/0203272.
31. Super-Kamiokande, M.B. Smy, hep-ex/0206016.
32. Soudan-2, W.W.M. Allison et al., Phys. Lett. B449 (1999) 137, hep-ex/9901024.
33. MACRO, M. Ambrosio et al., hep-ex/0304037.
34. G. Fogli et al., hep-ph/0303064.
35. A. Weber, hep-ex/0205043.
36. Y. Oyama, hep-ex/0210030.
37. LSND, A. Aguilar et al., Phys. Rev. D64 (2001) 112007, hep-ex/0104049.
38. MiniBooNE, A. Bazarko, hep-ex/0210020.
39. C. Giunti, C.W. Kim and M. Monteno, Nucl. Phys. B521 (1998) 3, hep-ph/9709439.
40. M. Apollonio et al., Eur. Phys. J. C27 (2003) 331, hep-ex/0301017.
41. F. Boehm et al., Phys. Rev. D64 (2001) 112001, hep-ex/0107009.
42. G.L. Fogli et al., Phys. Rev. D66 (2002) 093008, hep-ph/0208026.
43. S.M. Bilenky and C. Giunti, Phys. Lett. B444 (1998) 379, hep-ph/9802201.

44. W.L. Guo and Z.Z. Xing, Phys. Rev. D67 (2003) 053002, hep-ph/0212142.
45. S.M. Bilenky et al., Phys. Rept. 379 (2003) 69, hep-ph/0211462.
46. C. Weinheimer, hep-ex/0210050.
47. KATRIN, A. Osipowicz et al., hep-ex/0109033.